Can radar signals enhance thermal and optical bands for monitoring water status of olive trees?

Abdelhafid Elallaoui[1, 2*], *Saïd* Khabba[1, 3], *Nadia* Ouaadi[3], *Salah* Er-Raki[3,4], *Jamal* Ezzahar[1,3,5], *Pierre-Louis* Frison[2], *and Lionel* Jarlan[6]

[1]LMFE, Faculty of Sciences Semlalia, Cadi Ayyad University, Marrakech, Morocco
[2]LaSTIG, Gustave Eiffel University, Paris, France
[3]CRSA, Mohammed VI Polytechnic University, Ben Guerir, Morocco
[4]AgroBiotec Center, Faculty of Sciences and Techniques, Cadi Ayyad University, Marrakech, Morocco
[5]National School of Applied Sciences, Cadi Ayyad University (UCA), Safi, Morocco
[6]CESBIO, Centre d'Etudes Spatiales de la Biosphère, Toulouse, France

Abstract. In semi-arid regions, irrigation represents over 85% of water use, making its efficient management crucial. Accurate estimation of evapotranspiration (ETR) is essential to determine crop water requirements. The FAO-56 method, based on crop coefficient (K_c), is widely used for ETR estimation. While NDVI from optical data has been applied to estimate K_c, it shows limited variation for tree crops despite phenological changes. Radar data, however, are sensitive to structural vegetation changes at the wavelength scale. This study evaluates the capability of C-band radar data to estimate K_c for olive trees. Empirical relationships were assessed between K_c and temporal coherence (ρ) in VV and VH polarizations, as well as backscattering coefficients (σ^0) from Sentinel-1 over the 2021 seasonal cycle. A high agreement is observed between σ^0_{VV} and K_c, with a correlation coefficient of 0.76 and an RMSE of 0.11, highlighting the capability of radar data for improving evapotranspiration estimation in tree crops.

1 Introduction

In semi-arid environments, agriculture constitutes the main sector of freshwater consumption, reaching approximately 90% of overall water use [1, 2]. Under such conditions of water scarcity, improving the efficiency and sustainability of water management has become a major challenge. A detailed understanding of hydrological processes, particularly evapotranspiration (ETR), is therefore essential, since ETR constitutes the principal component of the water balance in dry and water-limited environments [3].

Actual evapotranspiration can be estimated through direct field measurement techniques, including eddy covariance and lysimeters instruments. These methods are known for their high accuracy; however, they are often costly to implement and generally restricted to limited spatial coverage [4]. As an alternative, evapotranspiration (ETR) can be estimated using land surface modeling approaches. These models differ in their structure and input requirements

* Corresponding author: a.elallaoui.ced@uca.ac.ma

and are designed to represent water fluxes, energy exchanges, or a combination of both, with varying levels of complexity [4].

Among these approaches, the FAO-56 methodology is widely used in irrigation studies due to its simplicity and relatively low data demand [5]. Its applicability has been demonstrated across different climatic zones and crop types, confirming its robustness [6]. Within this framework, crop evapotranspiration is computed by scaling the reference evapotranspiration (ET_0), which corresponds to a well-watered reference grass surface, using a crop coefficient (K_c) that accounts for the real physiological condition and development of the vegetation. Therefore, obtaining reliable K_c values is is crucial for optimizing irrigation scheduling and improving agricultural water use efficiency [6].

The value of K_c evolves during the growing cycle according to crop development stages and is influenced by several parameters, including irrigation strategy, vegetation cover fraction, cultivation practices, crop duration, and local environmental conditions. Satellite remote sensing has therefore become an important source of information for estimating K_c, particularly through vegetation indices derived from optical imagery. Among these indices, NDVI (Normalized Difference Vegetation Index) is extensively used, and numerous linear as well as nonlinear formulations have been proposed to relate NDVI to K_c [7, 8]. Despite their effectiveness, optical observations remain highly sensitive to atmospheric disturbances, especially cloud cover, which may considerably reduce image availability over long periods. This limitation is particularly critical for winter crops and for regions often affected by continuous cloud conditions. In the last decade, C-band Synthetic Aperture Radar (SAR) has seen growing use in vegetation monitoring, particularly after Sentinel-1A (2014) and Sentinel-1B (2016) were placed into orbit. Radar backscatter at C-band results from complex interactions between vegetation structure and soil properties. Nevertheless, previous studies have demonstrated that radar-derived parameters related to both signal amplitude and phase can provide valuable information on crop characteristics such as biomass, canopy density, and plant height.

The radar backscatter coefficient (σ^0), representing the intensity of the returned signal, is influenced simultaneously by vegetation and soil conditions. To minimize the influence of soil effects and soil–vegetation interactions, the polarization ratio ($PR=\sigma^0_{VH}/\sigma^0_{VV}$) has been introduced, where σ^0_{VH} and σ^0_{VV} correspond to cross-polarized and co-polarized backscatter signals, respectively. Previous investigations reported that this ratio exhibits greater temporal stability than backscatter intensity alone and can effectively capture seasonal biomass variations [9]. More recently, study [10] successfully applied this indicator for estimating crop coefficients in rice, sugarcane, and vegetable crops. Besides signal intensity, radar phase information has also shown strong sensitivity to crop development through temporal coherence (ρ) [9]. In this regard, [11] identified a direct relationship between temporal coherence and crop coefficient values for wheat, emphasizing the potential of SAR coherence for monitoring crop water requirements with improved accuracy.

This research explores whether radar observations can be employed to derive the FAO-56 crop coefficient as a substitute for optical and thermal data.

2 Data and Methodology

2.1 Study site and data

The experimental site is located within the Haouz plain, specifically in the Chichaoua province of central Morocco (Fig. 1). The site experiences a semi-arid climate marked by limited precipitation and elevated atmospheric water demand, with annual potential evapotranspiration values approaching 1600 mm [2]. According to the IPCC, the Haouz plain

is considered particularly vulnerable to climate change impacts [12]. Agricultural irrigation in the region relies predominantly on conventional practices, which have contributed to excessive pressure on groundwater reserves [13]. Approximately 2000 km² of the plain are irrigated, with cereal production occupying nearly 51% of this area and arboriculture accounting for about 38% [14]. The remaining 4000 km² mainly support rainfed wheat cultivation [14]. The investigated field covers nearly 2.4 ha and consists of an olive plantation organized into 40 rows containing 11 trees each, with an inter-tree spacing of 7.5 × 7.5 m². The olive trees are approximately 20 years old and reach an average height of 3 m. The orchard is established on clay-loam soil and supplied with water through a drip irrigation system. Soil composition in the study area is characterized by roughly 30% clay, 30% silt, and 40% sand [15].

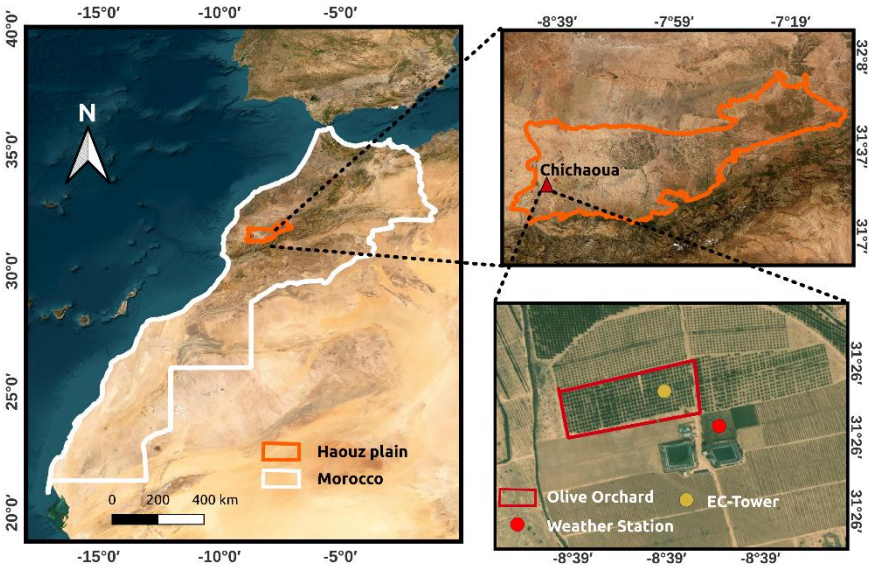

Fig. 1. Map showing the experimental olive orchard in central Morocco (Haouz Plain).

2.2 Climate Data Acquisition, Eddy Covariance System, and Crop Coefficient Calculation

At the experimental location, an automatic weather station was deployed to collect atmospheric measurements on a continuous basis. The recorded parameters included global solar radiation (R_g), wind speed (W), air temperature (T_{air}), and relative humidity (H_r), all sampled at 30-minute intervals. Real evapotranspiration (ETR) was estimated using an eddy covariance system equipped with a CSAT3 3D sonic anemometer and a KH20 krypton hygrometer.

Reference evapotranspiration (ET_0) refers to the water flux exchanged with the atmosphere from a hypothetical reference grass surface maintained under well-watered conditions. This standardized surface is defined by a height of 0.12 m, an albedo value of 0.23, and a surface resistance of 70 sm^{-1}. ET_0 is used to characterize the evaporative demand of the atmosphere independently of vegetation or soil properties. In this work, ET_0 was derived from meteorological data following the FAO-56 approach, based on the Penman–Monteith equation:

$$ET_0 = \frac{0.408\Delta(R_n - G) + \frac{\gamma 900}{T_{air} + 273} u_2 (e_s - e_a)}{\Delta + \gamma(1 + 0.34u_2)} \quad (1)$$

In this formulation, Rn (MJ/m²/day) represents the net radiation available at the crop surface, whereas G (MJ/m²/day) denotes the soil heat flux. Wind speed at 2 m height is given by u_2 (m/s), and T_{air} (°C) corresponds to the mean air temperature measured at the same reference height. The psychrometric constant is expressed as γ (kPa/°C). Saturation vapor pressure (e_s) and actual vapor pressure (e_a), both in kPa, are computed at 2 m above ground level. For daily calculations, the soil heat flux is generally assumed to be negligible. All remaining variables were derived from daily meteorological records according to the procedure described in [6].

The crop coefficient (K_c) was then obtained by dividing measured actual evapotranspiration (ETR) by the computed reference evapotranspiration (ET_0).

2.3 Sentinel-1 Radar Observations

The Sentinel-1 mission consists of two complementary satellites, Sentinel-1A and Sentinel-1B, launched in 2014 and 2016, respectively. Each platform carries a C-band Synthetic Aperture Radar (SAR) system operating at an approximate wavelength of 5.6 cm for Earth monitoring applications. Together, these satellites enable almost global coverage through 175 orbital paths and provide a revisit cycle of about six days. For terrestrial observations, data acquisition is generally carried out in Interferometric Wide Swath (IW) mode. This mode delivers dual-polarized imagery (VV and VH) over a swath width of about 250 km, with spatial resolutions close to 5 m in range and 20 m in azimuth direction. The present analysis focused on images acquired from descending orbit 52. Single Look Complex (SLC) products were employed for estimating temporal coherence (ρ), whereas Ground Range Detected (GRD) products were used to calculate the radar backscatter coefficient (σ^0). Temporal coherence was generated using a moving window of 15 × 3 pixels. All SAR processing steps were conducted using the ESA SNAP software package. Subsequently, the processed datasets were reprojected into the UTM Zone 29N coordinate reference system, and the reported values represent averages computed over the entire olive grove area.

3 Results

The relationships between K_c and the VV backscattering coefficient (σ^0_{VV}), the VH backscattering coefficient (σ^0_{VH}), and temporal coherence in VV (ρ_{VV}) and VH (ρ_{VH}) polarizations are presented in Fig. 2.

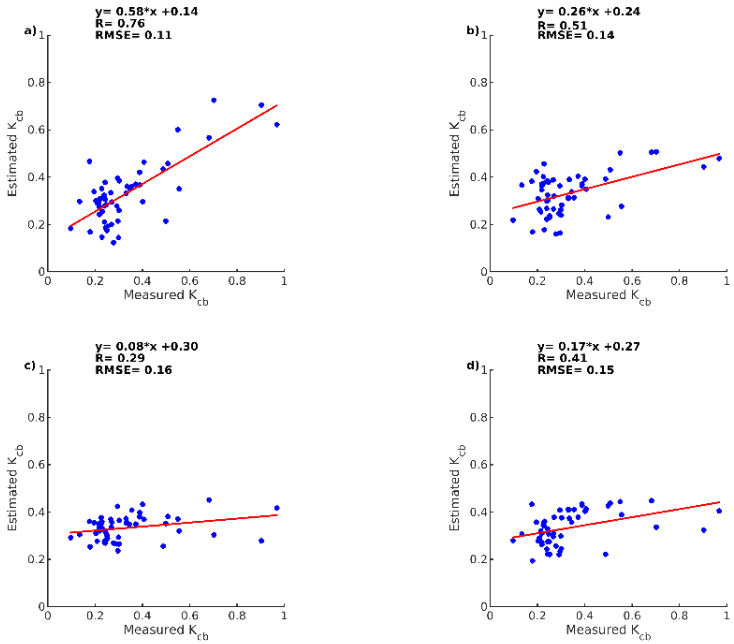

Fig. 2. Estimated versus measured K_c using the relationships: (a) $K_c - \sigma^0_{VV}$, (b) $K_c - \sigma^0_{VH}$, (c) $K_c - \rho_{VV}$, and (d) $K_c - \rho_{VH}$.

A linear regression approach was adopted to investigate the relationship between the crop coefficient (K_c) and radar-derived indicators, as these variables are commonly assumed to evolve proportionally with vegetation growth and canopy development. Under this assumption, a linear model provides an appropriate first-order representation of their relationship. The statistical analysis was carried out using a dataset composed of 53 paired observations. For each subplot, the fitted regression equation is presented together with the correlation coefficient (R) and the RMSE computed between measured K_c values and those estimated from the regression model (represented by the red line). The results indicate that the most significant relationship was observed between measured K_c and K_c estimated from σ^0_{VV}, with a correlation of 0.76 and an RMSE of 0.11. This stronger correlation can be explained by the high sensitivity of σ^0_{VV} to the overall canopy structure and water content of olive trees: as the canopy develops and becomes denser, both K_c and σ^0_{VV} increase in a consistent manner. Lower correlations were found for the other metrics, with values of 0.51, 0.29, and 0.41, and corresponding RMSE of 0.14, 0.16, and 0.15, for K_c estimated using σ^0_{VH}, ρ_{VV}, and ρ_{VH}, respectively. The weaker correlation observed for σ^0_{VH} is due to its dominance by volume scattering within the canopy, which is more sensitive to the internal arrangement of leaves and branches than to the overall canopy density that primarily controls K_c. The temporal coherence in VV and VH (ρ_{VV} and ρ_{VH}) shows weaker correlations because it does not capture a clear seasonal cycle for tree crops as it does for annual crops [11]. It is less sensitive to changes associated with canopy development and is more influenced by factors such as wind and small-scale canopy motion, which reduces its ability to reflect variations in K_c.

4 Conclusions

This work assessed the capability of C-band radar observations as an alternative to optical and thermal measurements for estimating the crop coefficient (Kc) in olive orchards. Among the tested radar variables, only the backscattering coefficient in VV polarization (σ^0_{VV}) showed a high correlation with K_c, with a correlation coefficient of 0.76 and an RMSE of 0.11. In contrast, the other radar-derived parameters exhibited moderate to weak correlations, with correlation coefficients of 0.51, 0.29, and 0.41 and corresponding RMSEs of 0.14, 0.16, and 0.15 for K_c estimates derived from σ^0_{VH}, ρ_{VV}, and ρ_{VH}, respectively. These results indicate that C-band radar data in VV polarization can provide reliable estimates of the basal crop coefficient and, consequently, crop evapotranspiration. However, the proposed relationships are specific to olive orchards under the conditions of the study area, and their applicability to other woody crops or different climatic contexts requires further investigation. This finding corroborates previous observations for wheat [11] and opens new perspectives for estimating actual evapotranspiration through the complementary use of radar, thermal, and optical data.

The experiment was conducted within the framework of the CNES-TOSCA MOCTAR project, with additional support from the International Joint Laboratory TREMA (https://www.lmi-trema.ma/). This research also benefited from the PRIMA-IDEWA and PRIMA-BIOMEnext projects. The authors acknowledge financial support from the RISE-H2020-ACCWA project (grant agreement No. 823965). The authors also thank Dr. O. Rafi, owner of the private farm where the experiment was performed.

References

1. S.S. Anapalli, D.K. Fisher, S.R. Pinnamaneni, K.N. Reddy, Quantifying evapotranspiration and crop coefficients for cotton (Gossypium hirsutum L.) using an eddy covariance approach. Agric. Water Manag. **233**, 106091 (2020). https://doi.org/10.1016/j.agwat.2020.106091
2. L. Jarlan, S. Khabba, S. Er-Raki, M. Le Page, L. Hanich, Y. Fakir, O. Merlin, S. Mangiarotti, S. Gascoin, J. Ezzahar, M.H. Kharrou, B. Berjamy, A. Saaïdi, A. Boudhar, A. Benkaddour, N. Laftouhi, J. Abaoui, A. Tavernier, G. Boulet, V. Simonneaux, F. Driouech, M. El Adnani, et R. Escadafal, Remote sensing of water resources in semi-arid Mediterranean areas: the joint international laboratory TREMA. Int. J. Remote Sens. **36**, 4879–4917 (2015). https://doi.org/10.1080/01431161.2015.1093198
3. J.E. Moorhead, Field-Scale Estimation of Evapotranspiration. In: Advanced Evapotranspiration Methods and Applications (IntechOpen, 2018). https://doi.org/10.5772/intechopen.80945
4. R.G. Allen, L.S. Pereira, T.A. Howell, M.E. Jensen, Evapotranspiration information reporting: I. Factors governing measurement accuracy. Agric. Water Manag. **98**, 899–920 (2011). https://doi.org/10.1016/j.agwat.2010.12.015
5. R.G. Allen, L.S. Pereira, D. Raes, M. Smith, Crop evapotranspiration—Guidelines for computing crop water requirements. FAO Irrigation and Drainage Paper No. 56 (FAO, Rome, 1998)
6. L.S. Pereira, P. Paredes, D.J. Hunsaker, R. López-Urrea, Z. Mohammadi Shad, Standard single and basal crop coefficients for field crops. Updates and advances to the FAO56 crop water requirements method. Agric. Water Manag. **243**, 106466 (2021). https://doi.org/10.1016/j.agwat.2020.106466
7. B. Duchemin, R. Hadria, S. Erraki, G. Boulet, P. Maisongrande, A. Chehbouni, R. Escadafal, J. Ezzahar, J.C.B. Hoedjes, M.H. Kharrou, S. Khabba, B. Mougenot, A. Olioso, J.C. Rodriguez, V. Simonneaux, Monitoring wheat phenology and irrigation in

Central Morocco: On the use of relationships between evapotranspiration, crop coefficients, leaf area index and remotely-sensed vegetation indices. Agric. Water Manag. **79**, 1–27 (2006). https://doi.org/10.1016/j.agwat.2005.02.013

8. S. Er-Raki, J.C. Rodriguez, J. Garatuza-Payan, C.J. Watts, A. Chehbouni, Determination of crop evapotranspiration of table grapes in a semi-arid region of Northwest Mexico using multi-spectral vegetation index. Agric. Water Manag. **122**, 12–19 (2013). https://doi.org/10.1016/j.agwat.2013.02.007
9. A. Elallaoui, P.-L. Frison, S. Khabba, A. Chakir, V. Le Dantec, S. Er-Raki, N. Ouaadi, P. Fanise, L. Villard, B. Fruneau, Z. Rafi, J. Ezzahar, and L. Jarlan, Assessment of the potential of sub-diurnal in situ C-band radar data for monitoring maize crop in semi-arid regions, Remote Sens. Environ., **336**, 115304 (2026). https://doi.org/10.1016/j.rse.2026.115304
10. S. Chintala, T.S. Harmya, B.V.N.P. Kambhammettu, S. Moharana, S. Duvvuri, Modelling high-resolution evapotranspiration in fragmented croplands from the constellation of Sentinels. Remote Sens. Appl. Soc. Environ. **26**, 100704 (2022). https://doi.org/10.1016/j.rsase.2022.100704
11. N. Ouaadi, L. Jarlan, S. Khabba, M. Le Page, A. Chakir, S. Er-Raki, P.-L. Frison, Are the C-band backscattering coefficient and interferometric coherence suitable substitutes of NDVI for the monitoring of the FAO-56 crop coefficient? Agric. Water Manag. **282**, 108276 (2023). https://doi.org/10.1016/j.agwat.2023.108276
12. IPCC, Climate Change 2022: Mitigation of Climate Change (IPCC, 2022)
13. Y. Ouassanouan, Y. Fakir, V. Simonneaux, M. Kharrou, H. Bouimouass, I. Najar, M. Benrhanem, F. Sguir, A. Chehbouni, Multi-decadal analysis of water resources and agricultural change in a Mediterranean semiarid irrigated piedmont under water scarcity and human interaction. Sci. Total Environ. **834**, 155328 (2022). https://doi.org/10.1016/j.scitotenv.2022.155328
14. B. Duchemin, O. Hoguet, B. Mougenot, I. Benhadj, R. Hadria, V. Simonneaux, J. Ezzahar, S. Hoedjes, M.H. Khabba, G. Kharrou, G. Boulet, S. Dedieu, R. Er-Raki, A. Escadafal, A. Olioso, Agrometeorological study of semi-arid areas: an experiment for analysing the potential of FORMOSAT-2 time series images in the Marrakech plain. Int. J. Remote Sens. **29**, 5291–5300 (2008). https://doi.org/10.1080/01431160802036482
15. H. Nassah, S. Er-Raki, S. Khabba, Y. Fakir, F. Raïbi, O. Merlin, B. Mougenot, Evaluation and analysis of deep percolation losses of drip irrigated citrus crops under non-saline and saline conditions in a semi-arid area. Biosystems Eng. **165**, 10–24 (2018). https://doi.org/10.1016/j.biosystemseng.2017.10.017